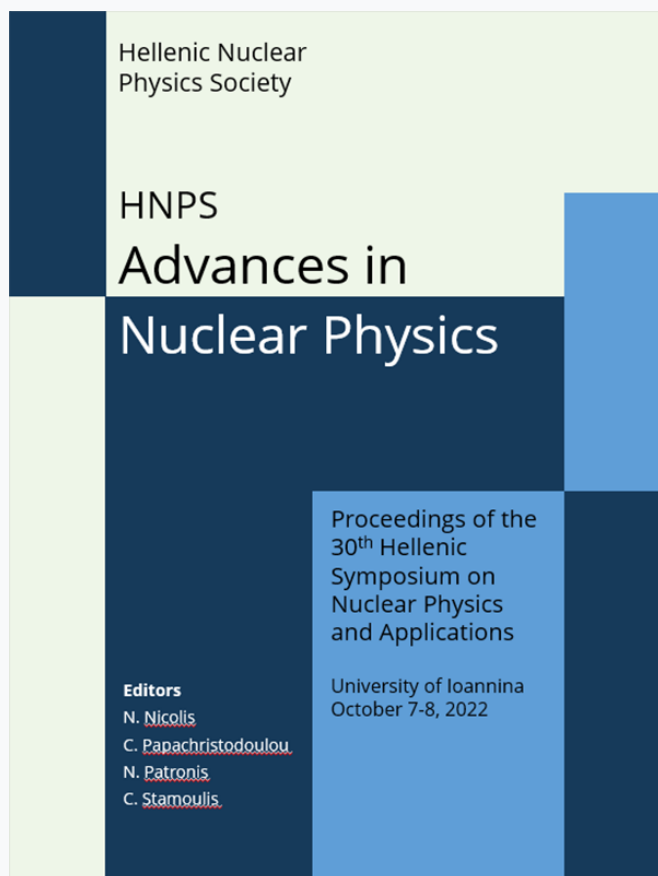


HNPS Advances in Nuclear Physics

Vol 29 (2023)

HNPS2022



Microscopic analysis of octupole shape phase transitions and critical points in neutron rich actinides

Vaia Prassa

doi: [10.12681/hnpsanp.5132](https://doi.org/10.12681/hnpsanp.5132)

Copyright © 2023, Vaia Prassa



This work is licensed under a [Creative Commons Attribution-NonCommercial-NoDerivatives 4.0](https://creativecommons.org/licenses/by-nc-nd/4.0/).

To cite this article:

Prassa, V. (2023). Microscopic analysis of octupole shape phase transitions and critical points in neutron rich actinides . *HNPS Advances in Nuclear Physics*, 29, 113–119. <https://doi.org/10.12681/hnpsanp.5132>

Microscopic analysis of octupole shape phase transitions and critical points in neutron rich actinides

Vaia Prassa*

Department of Physics, Faculty of Science, University of Thessaly, 3rd Km Old National Road Lamia -Athens, Lamia, 35100, Greece

Abstract Octupole constrained energy surfaces and spectroscopic observables of four isotopic chains of: Cm, Cf, Fm and No with neutron numbers $186 \leq N \leq 200$ are analysed using a collective quadrupole - octupole Hamiltonian (QOCH). The parameters of the Hamiltonian are determined by axially reflection-asymmetric relativistic Hartree-Bogoliubov calculations based on the energy density functional DD-PC1, and a finite-range pairing interaction. The theoretical results suggest quantum phase transitions from non-octupole to octupole deformed shapes and to octupole vibrations with increasing neutron number. ^{288}Cm is possibly close to the critical point of a simultaneous phase transition from spherical to prolate deformed and from non-octupole to stable octupole deformed configurations.

Keywords Relativistic density functionals, quadrupole-octupole collective Hamiltonian, octupole shapes, phase transitions

INTRODUCTION

The nuclear shape is one of the most extensively explored properties of atomic nuclei in low-energy nuclear physics, both experimentally and theoretically. The atomic nucleus is a many-body quantum system, and as such, the spontaneous symmetry breaking will cause the shape to be distorted from spherical and the nucleus to be deformed. The simplest shape distortion is quadrupole deformation with axial and reflection symmetry. Less often, nuclei are characterized by octupole “pear-like” shapes (stable or dynamical) due to spontaneous breaking of their intrinsic reflection symmetry. Reflection-asymmetric shapes in nuclei are due to the long-range octupole-octupole correlations that depend on the coupling of orbitals with $\Delta j = \Delta l = 3$ in the vicinity of the Fermi surface [1]. Regions of the nuclear chart that this condition is fulfilled are for proton Z and neutron numbers N close to 34, 56, 88, and 134 [1-4].

In the case of actinides ($Z \sim 96$ and $N \sim 196$), the coupling of the neutron orbitals $h_{11/2}$ and $k_{17/2}$, and that of the proton single-particle states $f_{7/2}$ and $i_{13/2}$, can lead to octupole deformations. Stable octupole deformation is characterized by the formation of the so called “octupole band” consisting of level sequences with alternating parities and enhanced electric dipole and octupole transitions. In the case of octupole vibrations, the negative-parity levels are systematically at higher energy than the ones in the γ -rast configuration, forming a separate collective band. In some regions of the nuclear chart, the evolution of the equilibrium shapes with the variation of nucleon number can be sudden and phenomena such as shape coexistence and quantum phase transitions may occur. Thorough theoretical and experimental efforts were performed investigating the phenomena of phase transitions in even-even nuclei near shell closures. Most of them focus on transitions between quadrupole collective degrees of freedom and only recently transitions from stable to dynamical octupole shapes have been considered. Nuclear structure models that have been used in theoretical studies of this type of transitions are algebraic (interacting boson) models (see for example in [6-8]), phenomenological collective models (see for example in [9-15]), cluster models (see for example [16-18]) and self-consistent mean-field models (see for example [19-26]).

* Corresponding author: vprassa@gmail.com

A systematic search for axial octupole deformation in the region of actinides and superheavy nuclei with proton numbers $Z = 88-126$ and neutron numbers from the two-proton drip line up to $N = 210$ within the covariant density functional theory (DFT) was performed in [24]. The existence of a region of octupole deformed nuclei around $Z \sim 96$ and $N \sim 196$ was confirmed in this study, in agreement with other studies in this region, based on the Skyrme DFT [27] and microscopic - macroscopic [28] calculations. In Ref. [25] reflection-asymmetric relativistic mean-field plus BCS (RMF+BCS) model, with the effective interaction in the particle-hole channel defined by the relativistic density functional PC-PK1 and an EDF-based quadrupole-octupole collective Hamiltonian was applied in a systematic analysis of octupole phase transition in eight neutron-rich isotopic chains - Ra, Th, U, Pu, Cm, Cf, Fm, and No.

In this work the axially reflection-asymmetric implementation of the relativistic Hartree-Bogoliubov (RHB) model [21, 23, 25], and the quadrupole-octupole collective Hamiltonian [21,23,31] constructed to calculate the excitation spectra and observables that can be related to quantum order parameters, are used. Shape phase transitions and critical points in the octupole deformed neutron-rich actinides: Cm, Cf, Fm and No are analysed and a microscopic realization of a QPT from non-octupole to stable octupole deformation and to octupole vibrations is presented. Calculations shown here have been partially presented in [41].

POTENTIAL ENERGY SURFACES AND SPECTROSCOPIC PROPERTIES

The RHB model provides a unified description of particle-hole (ph) and particle-particle (pp) correlations on a mean-field level. In the present analysis, the mean-field potential is determined by the relativistic density functional DD-PC1 [29] in the ph channel, and a separable pairing force [30] is used in the pp channel. The DD-PC1 functional has been successfully applied to various properties of finite nuclei, such as the phenomena of quantum phase transitions [32-34] and shape coexistence [35,36].

Already at the mean-field level, the RHB model predicts a very interesting structural evolution with transitions from non-octupole to pronounced octupole deformations and to shallow β_3 potentials (Fig. 1). In the case of ^{282}Cm , the potential energy surface (PES) is softer, with the energy minimum at $(\beta_2, \beta_3) \sim (0,0)$. With the increase of neutron number, more pronounced quadrupole and octupole deformations develop. For ^{288}Cm with $N=192$, the energy minimum is found in the non-zero octupole deformation region, located at $(\beta_2, \beta_3) \sim (0.09, 0.14)$. The potential becomes more rigid in β_2 and softer in β_3 . The maximum gain in binding energy due to octupole deformation $[\Delta E_{\text{oct}} = E^{\text{oct}}(\beta_2, \beta_3) - E^{\text{quad}}(\beta'_2, \beta'_3=0)]$, cf. Ref. [22,24] is found in ^{292}Cm at neutron number $N=196$.

To quantitatively study shape transitions and critical point phenomena, one must go beyond a simple Kohn-Sham approximation and take into account the restoration of broken symmetries at the mean-field level, and fluctuations in the collective coordinates. Spectroscopic properties relevant for the characterization of shape transitions are investigated using a quadrupole-octupole collective Hamiltonian that is a gamma rigid axially symmetric version of the general quadrupole-octupole Bohr Hamiltonian. The constrained self-consistent solutions of the relativistic Hartree-Bogoliubov equations at each point on the energy surface determine the mass parameters B_{22} , B_{23} , B_{33} , the three moments of inertia I_k , and the zero-point energy corrections as functions of the deformation parameters β_2 and β_3 . The moments of inertia are calculated according to the Inglis-Belyaev formula [37,38] and the mass parameters are calculated in the perturbative cranking approximation [23,39]. The collective potential is obtained by subtracting the zero-point energy corrections [39] from the total energy that corresponds to the solution of self-consistent mean field (SCMF) calculations. The diagonalization of the resulting Hamiltonian yields the low-energy excitation spectrum, collective wavefunctions, and reduced transitions probabilities of even-even nuclei.

Figures 2 and 3 display the systematics of the low-energy excitation spectra of the positive-parity

band ($K^\pi = 0^+_1$) and the lowest negative-parity band ($K^\pi = 0^-_1$), respectively, in the isotopic chains of Cm, Cf, Fm and No.

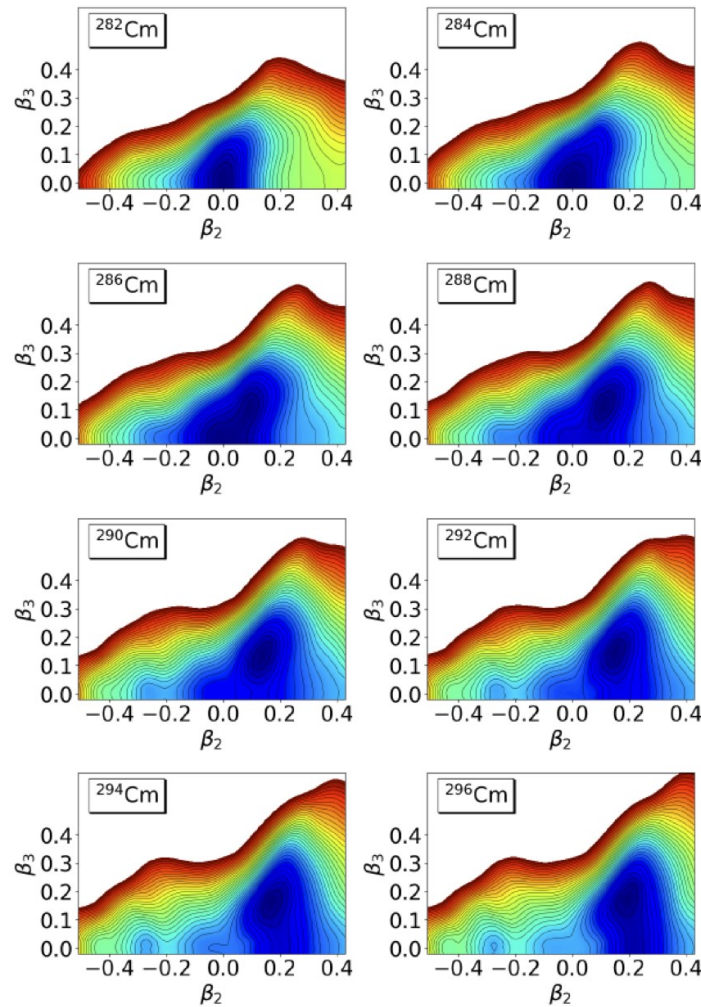


Figure 1. Microscopic DD-PC1 self-consistent relativistic Hartree-Bogoliubov axially symmetric energy surfaces of the nuclei $^{282-296}\text{Cm}$ in the (β_2, β_3) -plane. The contours join points on the surface with the same energy and the separation between neighboring contours is 0.5 MeV.

As shown in Fig. 2, the excitation energies of the $\pi = +$ even-spin states in the ground state band decrease with neutron number. The energy levels of isotopes with $N=186-190$ that are close to the neutron shell closure at $N=184$ are equidistant, indicating a quadrupole vibrational structure with $E(4^+_1)/E(2^+_1) \sim 2$, whereas for heavier nuclei with $N>194$, it is of rotational type $L(L+1)$ with $E(4^+_1)/E(2^+_1) \sim 3.33$. For all isotopes, the calculated excitation energies exhibit a pronounced decrease from $N=190$ to $N=192$, indicating the onset of increased quadrupole deformation. In the case of $^{288}\text{Cm}_{192}$, the $E(4^+_1)/E(2^+_1)$ ratio is equal to 2.7 which is close to the value 2.71 predicted by the $X(4)$ model introduced in Ref. [40], indicating a critical point of a quadrupole phase transition between spherical and quadrupole-deformed prolate shapes. The discrepancy could be due to missing triaxial correlations in the QOCH.

The calculated spectra of the $\pi = -$ odd-spin states as functions of N are shown in Fig. 3. Similarly to the positive-parity ground state energies [cf. Fig. 2] the calculated energy levels in the negative-parity band exhibit a sudden drop from $N=190$ to $N=192$, whereas for $N=192-196$ a weak dependence on neutron number is observed. A local minimum in the excitation spectra is observed in all isotopic chains that in Cm, Cf and Fm occurs at $N \sim 196$, while in No at $N \sim 192$. Starting from $N=198$ ($N=194$ in No), the energies of the $\pi = -$ odd-spin states systematically increase and the band becomes more compressed.

The results signify shape phase transitions from non-octupole to stable octupole deformations and to octupole vibrations as a function of the control parameter - the neutron number.

The relevant calculations using the quadrupole-octupole collective Hamiltonian based on the constrained self-consistent RMF+BCS solutions with the functional PC-PK1 and a δ -force pairing predict the minimum at neutron number $N \sim 198$ [25]. The discrepancies between the two theoretical results could be attributed to differences in the underlying shell structure and/or the different pairing strength in the two models.

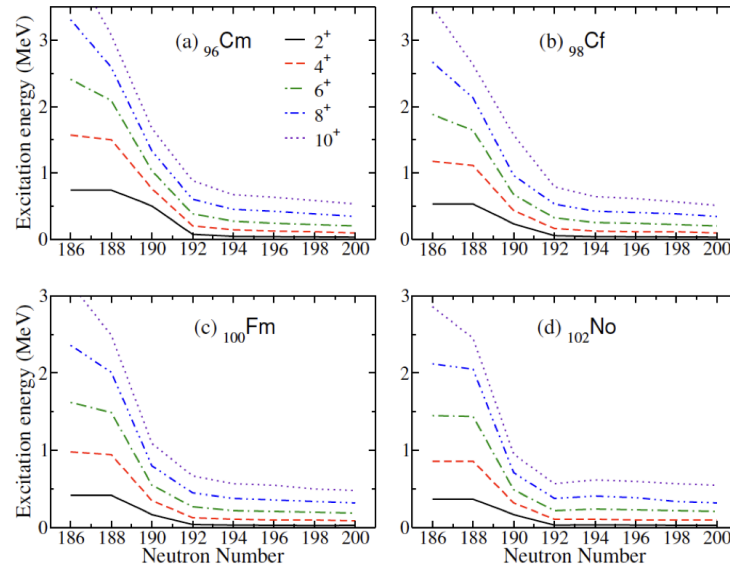


Figure 2. (Color online) Isotopic dependence of the excitation energies of levels of the positive-parity ground-state band $K^\pi = 0^+_1$ for (a) ${}_{96}\text{Cm}$, (b) ${}_{98}\text{Cf}$, (c) ${}_{100}\text{Fm}$, and (d) ${}_{102}\text{No}$.

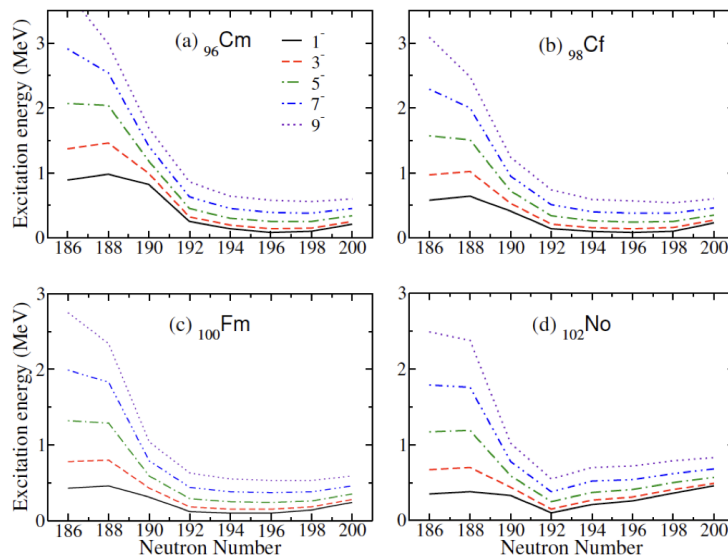


Figure 3. (Color online) Isotopic dependence of the excitation energies of levels of the negative-parity ground-state band $K^\pi = 0^-_1$ for (a) ${}_{96}\text{Cm}$, (b) ${}_{98}\text{Cf}$, (c) ${}_{100}\text{Fm}$, and (d) ${}_{102}\text{No}$.

Further evidence of the phase transitions from non-octupole to octupole deformation and octupole vibrations for shallow β_3 potentials is provided by the odd-even staggering in the energy ratio $E(J^\pi)/E(2^+_1)$ with $\pi = +$ for even-spin and $\pi = -$ for odd-spin yrast states. In the case of an alternating-parity rotational band, the energy ratio would depend quadratically on J . If the even-spin and odd-spin yrast states form a separate rotational band built on the octupole vibration, the ratio is expected to show

a pronounced odd-even-spin staggering. Figure 4 displays the ratios $E(J^\pi)/E(2^+)$ for both positive- and negative-parity yrast states of $^{282-296}\text{Cm}$, $^{284-298}\text{Cf}$, $^{286-300}\text{Fm}$ and $^{288-302}\text{No}$ as functions of the angular momentum J . One can see that in all isotopic chains the odd-even staggering is negligible for $N < 190$, with the $\pi=+$ and $\pi=-$ states lying close in energy meaning they merge into a single band. The staggering only becomes more pronounced starting at $N = 192$, indicating the onset of octupole vibrations that is the negative-parity band is a separate rotational band built on the octupole bandhead. The energy ratio $E(J^\pi)/E(2^+)$ for $\pi=-$ (odd-spin) states could be considered as an order parameter for the octupole shape transition.

A raise of the $B(E3; 3^- \rightarrow 0^+)$ transition rates is connected with increased octupole collectivity and is expected to be larger in octupole deformed nuclei. The isotopic dependence $B(E3; 3^- \rightarrow 0^+)$ reduced transition probabilities (in units W.u.) are shown in Fig. 5 for the isotopes of Cm, Cf, Fm and No. The theoretical values are obtained using the collective wave functions of $K^\pi = 0^+$ and $K^\pi = 0^-$ states from the QOCH calculation. The large $B(E3)$ values, shown in Fig.5, in all four isotopes with $N > 192$ indicate an enhanced octupole collectivity that is consistent with the emergence of octupole deformation at these neutron numbers in β_2 - β_3 energy surfaces [cf. Fig. 1]. In Cm, Cf and Fm isotopes, the higher $B(E3)$ values occur between $N=194$ and $N=198$ and in No at $N=192$ in consistency with the systematics of the calculated energy levels in the negative-parity band.

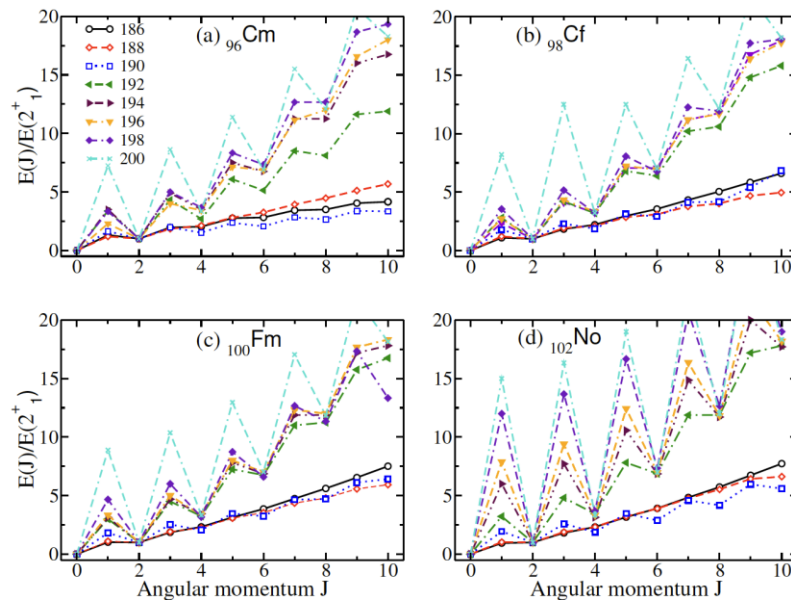


Figure 4. (Color online) Theoretical energy ratios $E(J^\pi)/E(2^+)$ of the yrast states of (a) ^{96}Cm , (b) ^{98}Cf , (c) ^{100}Fm , and (d) ^{102}No , including both positive (J even) and negative (J odd) parity, as functions of J .

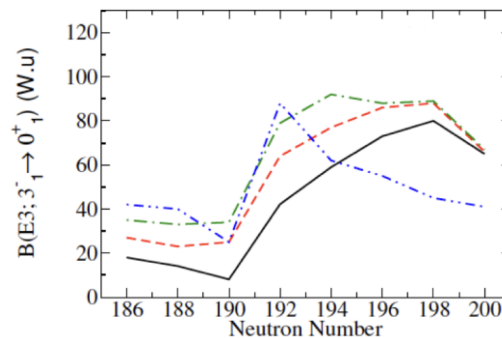


Figure 5. (Color online) Evolution of $B(E3; 3^- \rightarrow 0^+)$ values (in W.u. units) as functions of the neutron number in Cm, Cf, Fm and No isotopes.

CONCLUSIONS

Octupole collectivity and critical points of four isotopic chains of: Cm, Cf, Fm and No with neutron numbers $186 < N < 200$ have been investigated within the microscopic framework of nuclear DFT. Deformation constrained SCMF calculations have been performed with the relativistic Hartree-Bogoliubov method based on the universal energy density functional DD-PC1 and a separable pairing interaction. At the mean field level, the constrained β_2 - β_3 energy surfaces suggest phase transitions from non-octupole to octupole deformed shapes and to octupole vibrations with the critical points at neutron numbers at $N=192$ and $N=196$, respectively.

A collective quadrupole-octupole Hamiltonian with parameters determined by self-consistent mean-field calculations has been used to calculate the low-energy spectra of even-even isotopes. The energy levels of the positive-parity ground-state band of the isotopes under consideration exhibit a decrease with neutron number, manifesting a structural change from spherical vibrators to quadrupole deformed rotors. The states in the lowest negative-parity band display a parabolic dependence with increasing neutron number with the deepest minima at $N \sim 196$ in Cm, Cf, and Fm and $N=192$ in No that correspond to stable octupole deformations. The odd-even staggering, the probability density distributions for the ground states 0^+_1 and the 1^-_1 states and the calculated $B(E3)$ reduced transition probabilities confirm the structural change from spherical vibrators to deformed rotors and from octupole deformed configurations to octupole vibrators with increasing neutron number.

In the isotopic chain of Cm, the calculations signify the onset of a double phase transition from spherical to quadrupole-deformed and from non-octupole to octupole-deformed shapes, with ^{288}Cm being closest to the critical point. The neutron-rich actinides considered here appear to have a complex structure with octupole and triaxially deformed shapes. A more complete description of their properties would require extensions of the model in such a way that it simultaneously handles the reflection asymmetric degree of freedom and the triaxial deformation. Experimental studies in this region would help identify any deficiencies of the model, i.e. missing degrees of freedom, description of the underlying shell structure and/or pairing correlations.

References

- [1] P. A. Butler and W. Nazarewicz, *Rev. Mod. Phys.* 68, 349 (1996)
- [2] I. Ahmad and P. A. Butler, *Annu. Rev. Nucl. Part. Sci.* 43, 71 (1993)
- [3] P. A. Butler and L. Willmann, *Nucl. Phys. News* 25, 12 (2015)
- [4] P. A. Butler, *J. Phys. G: Nucl. Part. Phys.* 43, 073002 (2016)
- [5] P. Cejnar, J. Jolie, and R. F. Casten, *Rev. Mod. Phys.* 82, 2155 (2010)
- [6] J. Engel and F. Iachello, *Nucl. Phys. A* 472, 61 (1987)
- [7] N. V. Zamfir and D. Kusnezov, *Phys. Rev. C* 67, 014305 (2003)
- [8] K. Nomura, *Phys. Rev. C* 105, 054318 (2022)
- [9] D. Bonatsos, D. Lenis, N. Minkov, D. Petrellis, and P. Yotov, *Phys. Rev. C* 71, 064309 (2005)
- [10] D. Lenis and D. Bonatsos, *Phys. Lett. B* 633, 474 (2006)
- [11] R. V. Jolos, P. von Brentano, and J. Jolie, *Phys. Rev. C* 86, 024319 (2012)
- [12] N. Minkov, S. Drenska, M. Strecker, W. Scheid, and H. Lenske, *Phys. Rev. C* 85, 034306 (2012)
- [13] P. G. Bizzeti and A. M. Bizzeti-Sona, *Phys. Rev. C* 88, 011305(R) (2013)
- [14] D. Bonatsos, A. Martinou, N. Minkov, et al., *Phys. Rev. C* 91, 054315 (2015)
- [15] R. Budaca, P. Baganu, and A. I. Budaca, *Phys. Rev. C* 106, 014311 (2022)
- [16] F. Iachello and A. D. Jackson, *Phys. Lett. B* 108, 151 (1982)
- [17] H. J. Daley and F. Iachello, *Ann. Phys. (NY)* 167, 73 (1986)
- [18] T. M. Shneidman, G. G. Adamian, N. V. Antonenko, et al., *Phys. Rev. C* 67, 014313 (2003)
- [19] R. Rodriguez-Guzman, L. M. Robledo, and P. Sarriuren, *Phys. Rev. C* 86, 034336 (2012)
- [20] L. M. Robledo and P. A. Butler, *Phys. Rev. C* 88, 051302(R) (2013)
- [21] Z.P. Li, B.Y. Song, J.M. Yao, D. Vretenar, J. Meng, *Phys. Lett. B* 726, 866869 (2013)
- [22] S. E. Agbemava, A. V. Afanasjev, and P. Ring, *Phys. Rev. C* 93, 044304 (2016)
- [23] S. Y. Xia, H. Tao, Y. Lu, Z. P. Li, Niksic, and D. Vretenar, *Phys. Rev. C* 96, 054303 (2017)

- [24] S. E. Agbemava and A. V. Afanasjev, *Phys. Rev. C* 96, 024301 (2017)
- [25] Z. Xu and Z.-P. Li, *Chin. Phys. C* 41, 124107 (2017)
- [26] Y. Cao, S. E. Agbemava, A. V. Afanasjev, et al. *Phys. Rev. C* 102, 024311 (2020)
- [27] J. Erler, K. Langanke, H. P. Loens, et al., *Phys. Rev. C* 85, 025802 (2012)
- [28] P. Moller, J. R. Nix, W. D. Myers, and W. J. Swiatecki, *At. Data Nucl. Data Tables* 59, 185 (1995)
- [29] T. Niksic, D. Vretenar, and P. Ring, *Phys. Rev. C* 78, 034318 (2008)
- [30] Y. Tian, Z. Y. Ma, and P. Ring, *Phys. Lett. B* 676, 44 (2009)
- [31] Z. P. Li, T. Niksic, and D. Vretenar, *J. Phys. G* 43, 024005 (2016)
- [32] K. Nomura, T. Niksic, and D. Vretenar, *Phys. Rev. C* 96, 014304 (2017)
- [33] V. Prassa, T. Niksic, G. A. Lalazissis, and D. Vretenar, *Phys. Rev. C* 86, 024317 (2012)
- [34] V. Prassa, T. Niksic, and D. Vretenar, *Phys. Rev. C* 88, 044324 (2013)
- [35] V. Prassa, K.E. Karakatsanis, *Int. J. Mod. Phys. E* 30(07), 2150054 (2021)
- [36] Z. P. Li, T. Niksic, and D. Vretenar, *J. Phys. G: Nucl. Part. Phys.* 43, 024005 (2016)
- [37] D. R. Inglis, *Phys. Rev.* 103, 1786 (1956)
- [38] S. T. Belyaev, *Nucl. Phys.* 24, 322 (1961)
- [39] M. Girod and B. Grammaticos, *Nucl. Phys. A* 330, 40 (1979)
- [40] R. Budaca, A.I. Budaca, *Phys. Lett. B* 759, 349-353 (2016)
- [41] V. Prassa, *European Physical Journal A* 58(9), 183 (2022)